Solution Structure of Discrepin, a New K^+-Channel Blocking Peptide from the α-KTx15 Subfamily[†,‡]

Ada Prochnicka-Chalufour,[§] Gerardo Corzo,[||] Honoo Satake,[⊥] Marie-France Martin-Eauclaire,[@] Anna Rosa Murgia,[#] Gianfranco Prestipino,[#] Gina D'Suze,[+] Lourival D. Possani,[||] and Muriel Delepierre*[,§]

Unité de RMN des Biomolécules URA 2185 CNRS, Institut Pasteur, 28 Rue du Dr Roux, 75724 Paris Cedex 15, France, Department of Molecular Medicine and Bioprocesses, Institute of Biotechnology, National Autonomous University of Mexico, Avenida Universidad, 2001 Cuernavaca, 62210 Mexico, Suntory Institute for Bioorganic Research, 1-1-1 Wakayamadai, Shimamoto-Cho, Mishima-Gun, Osaka 618-8503, Japan, CNRS FRE 2738, Institut Federatif de Recherche Jean Roche, Faculté de Médecine Nord, Université de la Méditerranée, Bd Pierre Dramard, 13916 Marseille Cedex 20, France, Istituto di Biofisica, CNR, Via De Marini 6, 16149 Genova, Italy, and Instituto Venezuelano de Investigaciones Cientificas, Caracas, Venezuela

Received September 22, 2005; Revised Manuscript Received December 12, 2005

ABSTRACT: Discrepin, isolated from the venom of the Venezuelan scorpion *Tityus discrepans*, blocks preferentially the I_A currents of the voltage-dependent K^+ channel of rat cerebellum granular cells in an irreversible way. It contains 38 amino acid residues with a pyroglutamic acid as the N-terminal residue [D'Suze, G., Batista, C. V., Frau, A., Murgia, A. R., Zamudio, F. Z., Sevcik, C., Possani, L. D., and Prestipino, G. (2004) *Arch. Biochem. Biophys. 430,* 256−63]. It is the most distinctive member of the α-KTx15 subfamily of scorpion toxins. Six members of the α-KTx15 subfamily have been reported so far to be specific for this subtype of the K^+ channel; however, none of them have had their three-dimensional structure determined, and no information for the residues possibly involved in channel recognition and binding is available. Natural discrepin (n-discrepin) was prepared from scorpion venom, and its synthetic analogue (s-discrepin) was obtained by solid-phase synthesis. Analysis of two-dimensional ^{1}H NMR spectra of n- and s-discrepin indicates that both peptides have the same structure. Here we report the solution structure of s-discrepin determined by NMR using 565 meaningful distance constraints derived from the volume integration of the two-dimensional NOESY spectrum, 22 dihedrals, and three hydrogen bonds. Discrepin displays the α/*β* scaffold, characteristic of scorpion toxins. Some features of the proposed interacting surface between the toxin and channel as well as the opposite "α-helix surface" are discussed in comparison with those of other α-KTx15 members. Both n- and s-discrepin exhibit similar physiological actions as verified by patch−clamp and binding and displacement experiments.

K^+ channels play a critical role in a wide variety of physiological processes, including cell excitability, the regulation of heart beat rate, muscle contraction, neurotransmitter release, hormonal secretion, signal transduction, and cell proliferation (*2*). K^+ channels are a diverse superfamily of more than 80 members. For the purpose of hunting and defense, scorpions have evolved many different bioactive peptides, among which are toxins capable of blocking the function of K^+ channels. Thus far, more than 120 different K^+-channel toxins have been found in scorpion venoms (*3*). According to their primary structures and functions, they have been classified into three subfamilies, called α-, *β*-, and *γ*-Ktx (*4*), now extended to four subfamilies by the inclusion of *κ*-Ktx (see the review in ref *3*).

One of the less studied and least understood K^+ channels is that responsible for the A currents in the cerebellum granular cells, belonging to the voltage-gated Kv4 K^+ channels of the *Shal* subfamily (*2, 5*−*8*). These channels, also called fast transient K^+ channels (transient A), regulate firing frequency, spike initiation, and the waveform of action potential (*2, 6*). A-type K^+ currents result mainly from the expression of voltage-dependent Kv α-subunits (Kv1.4, -3.4, -4.1, -4.2, and -4.3) or from the coexpression of a Kv1 α-subunit together with a Kv *β*-subunit (*8*). Only a few blockers acting on these A-type K^+ channels have been identified and were extracted either from tarantula spider venom for fast transient K^+ channels (*5, 9*−*11*) or from sea anemones (*6, 12*). It has been shown that the phrixotoxins isolated from spiders blocked Kv4.2 and Kv4.3 channels without affecting other A-current-related channels (*9*), whereas the sea anemone blood depressing substance toxins selectively blocked the Kv3.4 channels (*12*). To the best of our knowledge, toxins specific for Kv1.4 channels have not been described. As often in the case of ionic channels, characterization of, searching for, and identification of new

[†] The 600 MHz NMR spectrometer was funded by the Region Ile de France and the Institute Pasteur. This work was partially supported by the Italian CNR and the Mexican CONACyT. Grants 40251-Q from CONACyT and IN206003 from DGAPA-UNAM given to L.D.P. are also acknowledged.

[‡] The atomic coordinates of the structure of s-discrepin have been deposited in the Protein Data Bank as entry 2AXK. Chemical shifts have been deposited in the BioMagResBank as entry 6924.

* To whom correspondence should be addressed. Telephone: 33 (0) 1 45 68 88 71. Fax: 33 (0) 1 45 68 89 29. E-mail: murield@pasteur.fr.

[§] Unité de RMN des Biomolécules URA 2185 CNRS.

[||] National Autonomous University of Mexico.

[⊥] Suntory Institute for Bioorganic Research.

[@] Université de la Méditerranée.

[#] CNR.

[+] Instituto Venezuelano de Investigaciones Cientificas.

10.1021/bi0519248 CCC: $33.50
Published on Web 01/21/2006

```
Aa1          ZNETNKKCQGGS-CASVCRRVIGVAAGKCINGRCVCYP
BmTx3A       ZVETNVKCQGGS-CASVCRKAIGVAAGKCINGRCVCYP
AmmTX3       ZIETNKKCQGGS-CASVCRKVIGVAAGKCINGRCVCYP
AaTx1        ZIETNKKCQGGS-CASVCRRVIGVAAGKCINGRCVCYP
AaTx2        ZVETNKKCQGGS-CASVCRRVIVVAAGKCINGRCVCYP
Discrepin    ZIDTNVKCSGSSKCVKICIDRYNTRGAKCINGRCTCYP
```

FIGURE 1: Sequence alignment of the α-KTx15 subfamily. Cysteines are colored red.

toxins active on these channels should be valuable for studying the role of these ion channels in neural and cardiac tissues since hardly anything has been done up to now to describe the residues involved in A-type K^+-channel recognition and binding (*8*). Recently, several toxins active on these K^+ channels have been isolated from scorpions. Figure 1 shows the amino acid sequences of the six toxins of the subfamily (α-KTx15) reported to be specific for this subtype of K^+ channel. They all have the N-terminal amino acid blocked by cyclization of the amino acid in position 1 (glutamic acid/glutamine) into pyroglutamic acid. Peptides from this subfamily thus far isolated and tested are not displaced by any scorpion toxin of the other subfamilies or by Na^+-channel specific toxins or chlorotoxin (*1*). Five members of the α-KTx15 subfamily discovered previously include Aa1 from *Androctonus australis* which is shown to block A-type K^+ currents in cerebellar granular cells (*13*), BmTX3 from *Buthus martensi* Karch (*6*) and AmmTX3 from *Androctonus mauretanicus mauretanicus* which are found to block A-type current in striatal neurons (*7*), and AaTx1 and AaTx2 from the *A. australis* putative isoform of Aa1 (*14*). They all share a very high degree of sequence similarity (up to 98%). Discrepin, the sixth member of this subfamily, with systematic number α-KTx15.6 (*1*), displays only ∼50% sequence identity with the remaining members of the subfamily (see Figure 1) and ∼30% with toxins of other α-KTx subfamilies.

Here we describe the solution structure of s-discrepin, a 38-amino acid peptide cross-linked by three disulfide bridges. Pairings of cysteines at positions 8 and 29, 14 and 34, and 18 and 36 correspond to the usual pattern found in short chain scorpion toxins. Discrepin proton assignments and the secondary structure were determined for both the synthetic and the native toxin. As these indicated that both molecules have effectively the same structure, the three-dimensional structure of discrepin was obtained from data on the synthetic toxin, available in larger amounts. This is the first structure of a peptide of the α-KTx15 subfamily that affects potassium channels to be determined.

MATERIALS AND METHODS

Materials

Phenol, imidazole, thioanisole, 1,2-ethanedithiol, and trifluoroacetic acid (TFA) were purchased from Sigma-Aldrich Corp. (St. Louis, MO). All other chemicals and HPLC solvents were of analytical grade.

Peptide Synthesis

Synthetic discrepin (s-discrepin) was chemically synthesized on the solid phase using fluoren-9-ylmethoxycarbonyl (Fmoc) methodology on an Applied Biosystems 433A peptide synthesizer. Fmoc-Pro-TrtA-PEG resin (Watanabe Chemical Industries, Ltd., Hiroshima, Japan) and pyro-

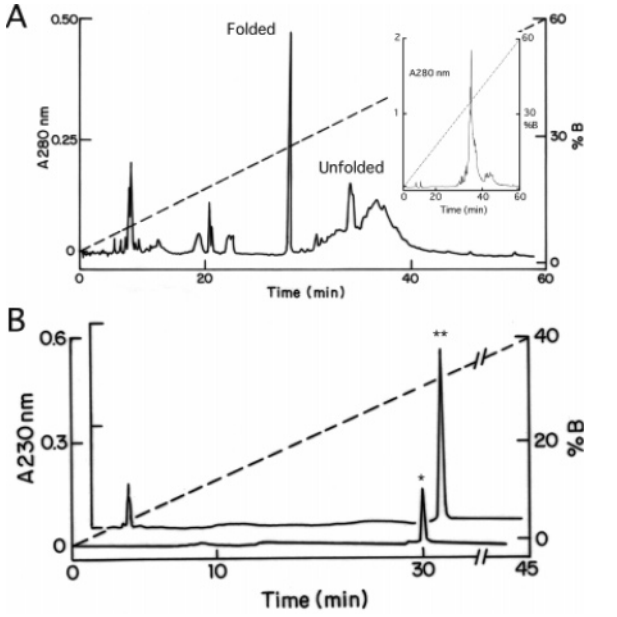

FIGURE 2: Reverse-phase HPLC separation of s-discrepin. (A) HPLC chromatogram after oxidation of s-discrepin. The inset is a HPLC chromatogram of the crude peptide before oxidation. (B) Reverse-phase chromatogram of s-discrepin (*) and coelution of both native and synthethic discrepin (**). Please note the shift on the time scale.

glutamic acid (Peptide Institute Inc., Osaka, Japan) were used to produce the C- and N-terminal residues of the protein, respectively. Cleavage, deprotection of peptide from the resin, and its deprotection were performed as described previously (*15*). The crude linear synthetic peptides were purified by RP-HPLC (Waters 600, with dual wavelength detector model 2847, Milford, MA) on a semipreparative C_{18} column (5C18MS, 10 mm × 250 mm, Nacalai Tesque) to 90−95% homogeneity, to eliminate synthetic byproducts and incorrectly assembled peptides using a 60 min linear gradient from 0 to 60% aqueous acetonitrile with 0.1% TFA (2 mL/min). The six free cysteine residues were allowed to oxidize in air for 24 h at room temperature in a 0.2 M aqueous Tris-base solution containing 1 mM reduced glutathione and 0.1 mM oxidized glutathione at pH 8.0. The folded synthetic toxins were purified on the same semipreparative C_{18} RP-HPLC column using the same gradient protocol indicated above and in the legend of Figure 2. The composition identity between synthetic and native peptides was verified by HPLC coelution experiments on an analytical C_{18} column (4.6 mm × 250 mm, Vydac, Hysperia, CA) using a 45 min linear gradient from 0 to 40% aqueous acetonitrile with 0.1% TFA (1 mL/min). Additionally, the mass identity between synthetic and native peptides was verified by electrospray ionization mass spectrometry using a Finnigan (San Jose, CA) LCQ^{DUO} ion trap mass spectrometer. The recovery yield of the synthetic peptides was 31.4 and 9% for the linear and oxidized forms, respectively.

NMR Structure Determination

Sample Preparation. Native discrepin (n-discrepin) was isolated from the venom of the Venezuelan scorpion *Tityus discrepans* (*1*). Its amino acid sequence was obtained by direct Edman degradation. Native discrepin, ∼200 μg of lyophilized powder, was dissolved first in 160 μL of a 9:1

(v/v) H_2O/D_2O mixture (Eurisotop). The sample concentration was at most 0.25 mM but probably less, and the pH of the solution was ~3. Then, 2 mg of lyophilized synthetic discrepin (s-discrepin) was dissolved in 160 μL of a 9:1 H_2O/D_2O mixture for the experiments using a 3 mm Shigemi tube leading to a sample concentration of 3 mM at pH 3. For experiments in D_2O, the sample was freeze-dried and then dissolved in D_2O.

NMR[1] *Experiments.* ^{1}H NMR experiments were performed on a 14T Varian Inova spectrometer using a 5 mm bore diameter pulse field gradient cryoprobe (Varian). The spectral width was 4500 or 6000 Hz for experiments in D_2O or H_2O, respectively. Proton chemical shifts were given relative to the 2,2-dimethyl-2-silapentane-5-sulfonic acid (DSS) as an external reference. Experiments were carried out at 25, 30, and 35 °C. The 2D ^{1}H NMR spectra were recorded in the phase sensitive mode (*16*) using experiments such as DQF-COSY (*17*, *18*), 2Q-COSY (*19*), TOCSY (*20*), and NOESY (*16*, *21*). The double-quantum experiment was optimized for a 15 Hz coupling constant. Clean TOCSY (*20*) spectra were acquired using the MLEV-17 sequence (*22*, *23*) with a mixing time of 70 ms. NOESY spectra were obtained with mixing times of 150, 200, and 250 ms. Distance constraints were obtained from NOESY spectra recorded in H_2O with a mixing time of 250 ms at 35 °C. Additional distance constraints, in particular those involving the aromatic protons and the Hα protons, were obtained from a NOESY spectrum recorded in D_2O at 35 °C with mixing times of 150 and 250 ms.

$^3J_{NH-H\alpha}$ coupling constants were measured directly from the one-dimensional spectrum obtained at different temperatures to overcome the problem of signal overlap, with a digital resolution of 0.18 Hz per data point after one zero filling. Main chain amide proton temperature coefficients of s-discrepin were calculated from chemical shifts determined on TOCSY experiments at temperatures increasing from 15 to 35 °C in steps of 5 °C. Hydrogen exchange rates were evaluated by freeze-drying the s-discrepin sample from H_2O and dissolving it in D_2O. One-dimensional experiments were carried out 30 min and 6 h after D_2O addition, and then TOCSY and NOESY experiments were carried out to identify the most slowly exchanging protons. This allowed grouping of the NH protons into three classes: the fast exchanging that disappeared after 30 min, the slowly exchanging observed in the 2D TOCSY experiment, and the remaining NH protons falling into the intermediate exchange rate class. Chemical shift index (CSI) prediction of secondary structure was performed using CSI software (*24*, *25*). Assignment of signals to peptide protons was achieved according to the standard method developed by Wüthrich and co-workers (*26*).

Experimental Restraints and Structural Calculation

Structures were calculated from data on the synthetic peptide obtained at 35 °C using NOE-derived distance constraints, Φ angle constraints issued from $^3J_{NH-H\alpha}$ coupling constants, and hydrogen bonds. Distance constraints were obtained from the NOESY spectra recorded in H_2O at 35 °C, with a mixing time of 250 ms, and analyzed with VNMR (VarianInc) and XEASY (*27*). $^3J_{NH-H\alpha}$ coupling constants were converted into dihedral angle constraints following the rule: $-65 \pm 40°$ for $^3J_{HN-H\alpha} \leq 5.5$ Hz and $-120 \pm 40°$ for $^3J_{HN-H\alpha} \geq 8.0$ Hz. Mass spectrometry analysis carried out on a reduced sample of discrepin indicated the presence of three disulfide bridges (*1*). Their arrangement based on sequence comparison was originally assumed to be between pairs of cysteine residues at positions 8 and 29, 14 and 34, and 18 and 36. Moreover, they were confirmed by NOE interactions observed between Hα and Hβ protons or between Hβ protons of paired cysteines. Hydrogen bonds that were present in 80% of all structures calculated beforehand without any hydrogen bond constraint and remaining in agreement with amide exchange data and with amide temperature coefficients were used as additional input data in final runs of calculations.

Structure calculation was combined with automatic NOE cross-peak assignment using ARIA version 1.2 (*28*) and CNS version 1.1 (*29*). Several cycles of ARIA were performed using standard protocols and by varying the chemical shift tolerance between 0.03 and 0.02 ppm. After each cycle rejected restraints, assignments and violations were analyzed; comparison with D_2O NOESY spectrum peaks was sometimes useful for verification of assignments. Finally, 400 conformers were calculated with ARIA/CNS, and the 40 structures with the lowest restraint energy values were refined in water. The ten best structures were used for statistical analysis. The structures were visualized and analyzed with MOLMOL (*30*), and their quality was assessed using PROCHECK (*31*) and WHATCHECK (*32*).

Molecular Modeling

Three-dimensional models of Aa1 and BmTX3 α-Ktx15 toxins were built with Modeller 6v2 (*33*). These are the most dissimilar sequences best representing the α-KTx15 subset without taking discrepin into account. The atomic structures of the following toxins available in the Protein Data Bank (*34*) were used as templates for comparative modeling: 1HP2, 1BIG, 2BMT, 2CRD, 2KTX, 1WMT, and 1AGT for both toxins; 1SXM, 1LIR, and 1SCO for Aa1; and 1BKT for BmTX3. The quality of models was assessed using PROCHECK (*31*).

Radioiodination of BmTX3

BmTX3 was radiolabeled by the lactoperoxidase method, as previously described (*6*). It was then desalted by HPLC before use. Matrix-assisted laser desorption ionization time-of-flight mass spectrometry (MALDI-TOF MS) analysis was performed on a Voyager-DE RP BioSpectrometer Workstation (Perseptive Biosystems) in the positive linear mode (*7*) to ensure that the derivatives were monoiodinated. Specific radioactivities of 2200 Ci/mmol were routinely obtained.

Pharmacological Tests on Rat Brain Synaptosomes

Rat brain synaptosomal fraction P2 was used for binding assays as described previously (*6*). The binding buffer consisted of 20 mM Tris-HCl, 50 mM NaCl, and 0.1% BSA (pH 7.2). Briefly, 20 μL of 0.4 nM [^{125}I]BmTX3 was

[1] Abbreviations: NMR, nuclear magnetic resonance; 2D, two-dimensional; NOE, nuclear Overhauser effects; NOESY, NOE spectroscopy; COSY, correlated spectroscopy; TOCSY, total correlated spectroscopy; DQ-COSY, double-quantum spectroscopy; rmsd, root-mean-square deviation; SA, simulated annealing; ChTX, charybdotoxin.

incubated with 20 μL of a series of concentrations (final concentration from 10^{-7} to 10^{-3} M) of the toxins tested and 90 μg of P2 by assay in a total volume of 200 μL. Nonspecific binding was assessed in the presence of 0.1 μM BmTX3. Incubation was carried out for 1 h at room temperature. The reaction was stopped by centrifugation of the mixture at 13000*g* for 3 min, and the pellet was washed twice with 1 mL of washing buffer, made of 20 mM Tris-HCl, 150 mM NaCl, and 0.1% BSA (pH 7.2). The radioactivity associated with the pellet was determined in a Packard γ-spectrometer (RIASTAR).

Competitive Liquid-Phase Radioimmunoassay (RIA)

Immune serum against BmTX3-delYP was obtained from New Zealand rabbits as described previously (*35*). A competitive liquid-phase RIA between [^{125}I]BmTX3 and discrepin was performed as follows. Fifty microliters of 0.4 nM [^{125}I]BmTX3 was incubated with 50 μL of a series of concentrations (final concentration from 10^{-7} to 10^{-11} M) of toxins tested and 100 μL of specific immune serum (1:300000 final concentration, v/v) or nonimmune serum (1:300 final concentration, v/v) as a control for 90 min at 37 °C; 300 μL of 50 mM phosphate buffer (pH 7.4) and 3% BSA was added before overnight incubation. Fifty microliters of 1:10 (v/v) anti-rabbit and 50 μL of 1:50 (v/v) nonimmune serum were added, and the sample was incubated for 90 min at 4 °C; 400 μL of 50 mM phosphate buffer containing 12% PEG was added, and the samples were incubated for 90 min at 4 °C. Complexes between ^{125}I-labeled toxins and their specific antibodies were precipitated by centrifugation at 11000*g* for 20 min. Then, the radioactivity of the pellet was counted.

Electrophysiological Measurements

Cell Culture. Experiments were performed on cerebellum granular cells in primary culture obtained from 8-day-old Wistar rats. Dissociated cell cultures were prepared by trypsin digestion and mechanical trituration, following the procedure of Levi et al. (*36*). Cells were plated at a density of 2.5×10^6 per dish, on 35 mm plastic dishes or on glass coverslips, coated with 10 mg/mL poly-L-lysine and kept at 37 °C in a humidified 95% air/5% CO_2 atmosphere. Experiments were performed 5−12 days after plating.

Patch−Clamp Measurements. Ionic currents were recorded in the whole-cell patch−clamp technique configuration (*37*). Patch pipets were made from borosilicate glass (CLARK Electromedical Instruments) and fire polished to obtain resistances between 2 and 4 MΩ. Cell responses were amplified and filtered at 2 kHz by an AxoPatch-1D instrument (Axon Instruments). Both stimulation and data acquisition were performed with a 16-bit AD/DA converter (DigiData 1200, Axon Instruments) controlled by a PC 486 computer. The whole-cell currents elicited by 150−200 ms voltage steps between −60 and 80 mV and between −50 and −80 mV holding potentials (HP) were acquired at a sampling time of 200 μs. The capacitive transient component and the series resistance of recorded currents were analogically compensated. P/4 leakage subtraction was performed on line. The composition of the pipet filling solution was as follows: 90 mM KF, 30 mM KCl, 2 mM $MgCl_2$, 2 mM EGTA, 5 mM NaCl, 30 mM glucose, and 10 mM HEPES buffer (pH 7.35). The external standard solution, designed to suppress Na^+ and Ca^{2+} currents, consisted of 135 mM NaCl, 2.5 mM KCl, 1 mM $MgCl_2$, 1.8 mM $CaCl_2$, 0.3 mM tetrodotoxin, 0.2 mM $CdCl_2$, 10 mM glucose, and 10 mM HEPES buffer (pH 7.35). Synthetic discrepin was directly added into the chamber containing 200 μL of external solution. All experiments were carried out at room temperature (23 ± 2 °C).

RESULTS

Chemical Synthesis and Proper Folding of Discrepin. The overall assembly and cleavage yield from the insoluble resin of synthetic discrepin was 54% according to theoretical values of the peptidyl resin and the calculated mass increase for 0.1 mmol of peptide to give 225.8 mg of crude synthetic peptide. The final yield after chromatographic purification of the linear peptide and refolding was ca. 9%. The chemically synthesized discrepin was shown to coincide with the native one by mass spectrometric analysis, biological activities, and similar coelution assays using reversed-phase HPLC (Figure 2).

Since the chemical synthesis of discrepin showed that the product obtained had the expected molecular mass and eluted in the HPLC system at the same position as the natural peptide, directly purified from the soluble venom of *T. discrepans*, further biological assays (electrophysiological and biochemical experiments) were performed to verify that similar physiological effects were obtained for both n- and s-discrepin. The small amount of n-discrepin available and the abundant s-discrepin were both used for structure determination, as presented below.

NMR Assignments. The sequence specific assignment of s- and n-discrepin was achieved according to a standard procedure (*26*). Spectra for assignments were recorded at three different temperatures, namely, 25, 30, and 35 °C, to solve ambiguities due to overlapping signals.

First, the spin systems of all amino acid residues were identified via their through-bond connectivity observed in COSY, TOCSY, and double-quantum experiments. Via a combination of the through-bond information acquired at several temperatures, all spin systems could be identified. Almost all protons were identified and their resonance frequencies determined.

Aromatic ring protons were assigned using TOCSY and COSY correlations in the aromatic region and specifically assigned from the NOEs observed between ring protons and Hβ and Hα protons in NOESY spectra collected in D_2O. The sequential assignment was then performed using the through-space connectivity observed between neighboring residues in the NOESY spectra. The sequential amide or Hα proton NOE connectivities of Tyr37 with the Hδ protons of Pro38 indicate that the Xaa−Pro amide bond is in the trans conformation. The chemical shifts of all protons of n- and s-discrepin are listed in Table S1 of the Supporting Information.

Structure of Discrepin. The NOE data that characterize the secondary structure of proteins, $^3J_{NH-H\alpha}$ coupling constants, amide exchange data, amide temperature coefficients, and Hα chemical shift data are summarized in Figure 3.

The structures were calculated with a total of 565 meaningful distance constraints derived from the volume integration of the 2D NOESY spectrum, 22 dihedrals, and

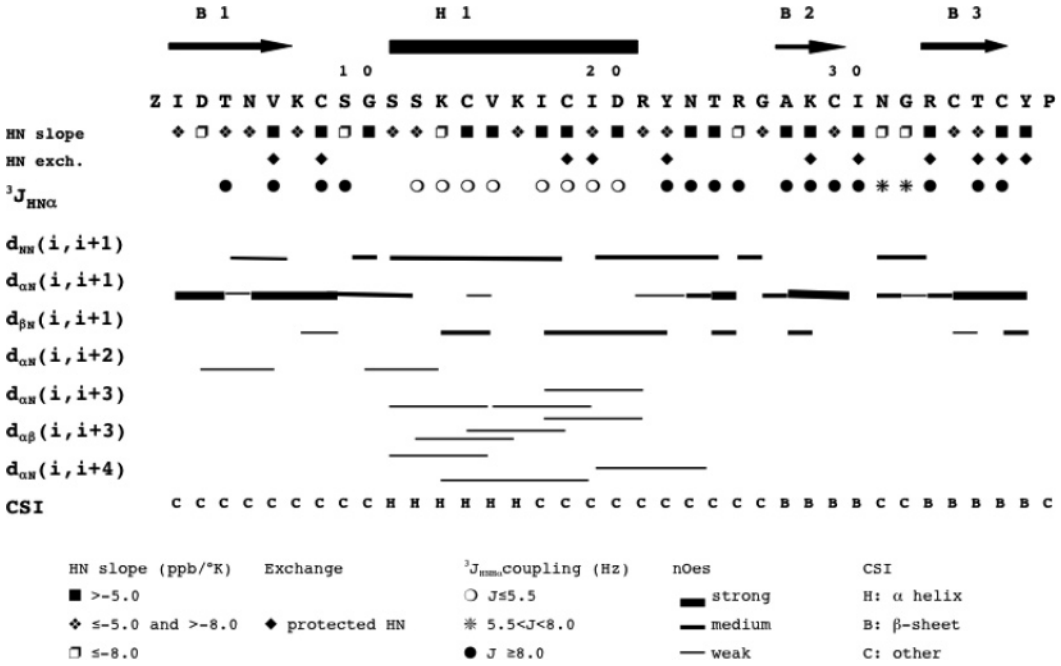

FIGURE 3: Summary of secondary structure NOE-related connectivities, amide exchange and temperature coefficient data, $^3J_{HN-N\alpha}$ coupling constants, and CSI (chemical shift index) predictions (*24*). The secondary structure elements determined from the final structures are shown above the sequence.

Table 1: Structural Statistics for the Ensemble of 10 Conformers Calculated for Discrepin

parameter	value
no. of constraints	
unambiguous	
intraresidue	246
sequential	95
medium-range	46
long-range	68
ambiguous	
intraresidue	30.7
sequential	22.9
medium-range	19.8
long-range	37.6
total	
intraresidue	276.7
sequential	117.0
medium-range	65.8
long-range	105.6
residual distance constraint violations	
≥0.3 Å	0
≥0.1 Å	13.3 ± 2.8
rmsd from NOEs (Å)	0.03 ± 0.002
no. of dihedral angle constraints	22
residual dihedral angle constraint violations	
≥5°	0
rmsd from dihedrals (deg)	0.6 ± 0.2
energies (kcal/mol)	
total	−1132 ± 45
van der Waals	−292 ± 7
electrostatic	−1265 ± 33
mean pairwise rmsd (Å) for all residues	
backbone atoms	0.7 ± 0.1
heavy atoms	1.4 ± 0.2
ensemble Ramachandran plot (%)	
residues in the most favored region	79.4 ± 1.9
residues in additionnally allowed regions	17.0 ± 1.6
residues in generously allowed regions	3.0 ± 0.5
residues in disallowed regions	0.9 ± 0.5

three hydrogen bonds. The three disulfide bonds established previously were used in all calculations. The details of the constraints used and the structural characteristics of the

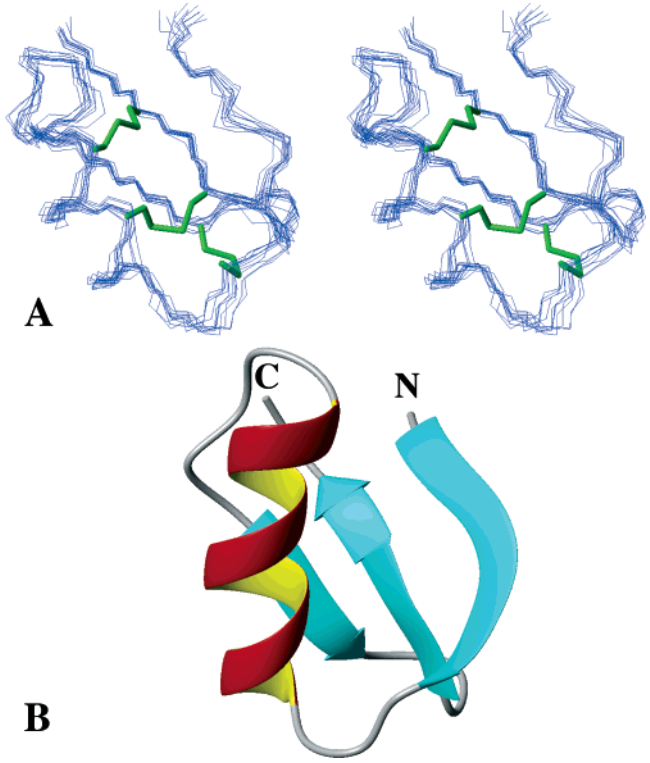

FIGURE 4: Structure of discrepin. (A) Stereoview of the backbone superposition of the 10 selected conformers. Disulfide bridges are colored green. (B) Ribbon representation of the best conformer showing the α-helix in red (residues 11−21) and the triple-stranded β-sheet in cyan (residues 2−7, 27−29, and 33−36). N and C denote the N- and C-termini, respectively.

family of 10 conformers are summarized in Table 1. The structures are in good agreement with the standard covalent geometry, and 96% of their ϕ and ψ dihedral angles belong to the most favored and allowed regions of the Ramachandran plot. No violations greater than 0.3 Å or 5° are observed for distance or angle constraints, respectively. The structures

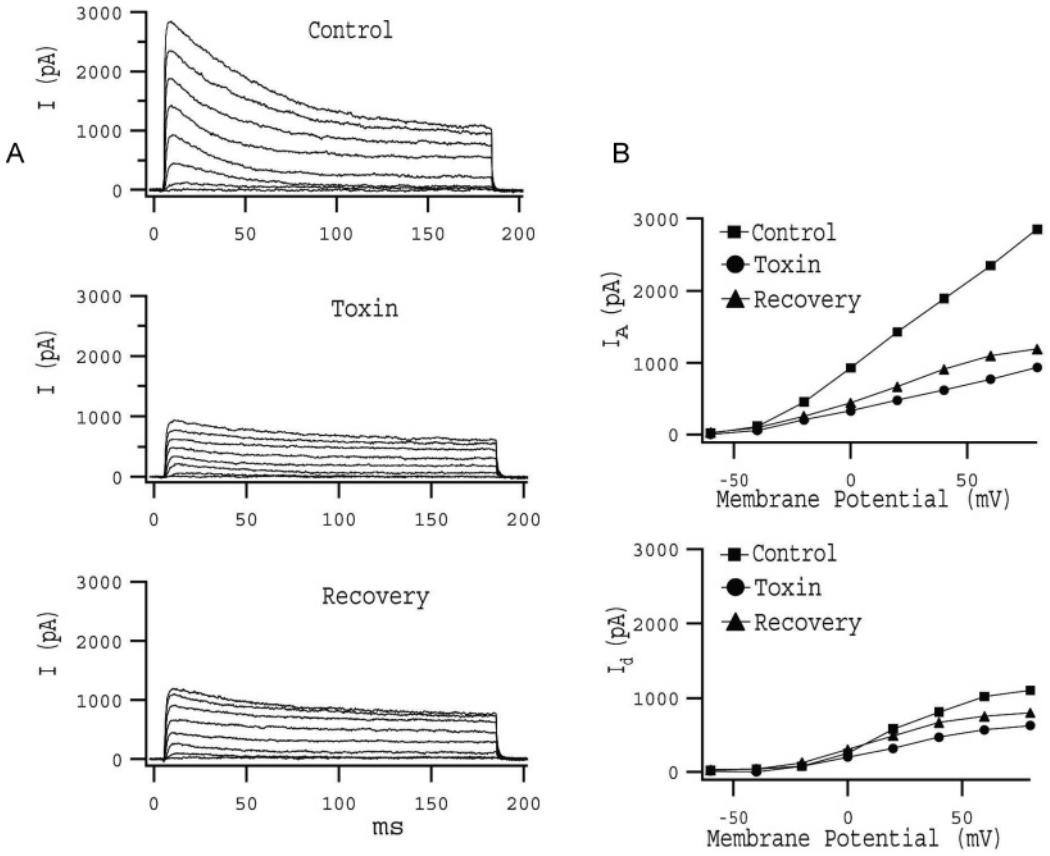

FIGURE 5: Electrophysiological experiments. (A) Effect of s-discrepin scorpion toxin on cerebellum cell outward K^+ currents. Toxin irreversibly blocks macroscopic K^+ currents at a concentration of 400 nM. The top traces are control K^+ currents elicited by voltage steps from −60 to 80 mV with 20 mV increments from a HP of −80 mV; the middle traces are the currents measured after the addition of discrepin to the external solution, and the bottom traces are those recorded after extensively perfusing the cell with the control external solution. (B) Current−voltage relationship for I_A and I_d currents under control conditions, in the presence of s-discrepin and after recovery with a control solution. Experimental points for I_A currents are measured at the peak value, while those for steady-state I_d currents are measured at the end of the 200 ms pulse.

display a good convergence, with mean pairwise rmsds of 0.7 ± 0.1 and of 1.4 ± 0.2 Å for all the backbone and heavy atoms, respectively.

Discrepin displays the α/β fold characteristic of scorpion toxins (Figure 4). The α-helix extends from residue Ser11 to Arg21. The antiparallel β-sheet is composed of three strands formed by residues Ile2−Lys7, Ala27−Cys29, and Arg33−Cys36, the first strand being distorted by a bulge comprising residues between Thr4 and Lys7.

Furthermore, direct NMR data suggest that the turn connecting the first β-strand to the α-helix can be characterized as a type II′ β-turn and the last one, running between the second and the third antiparallel β-strands, as a type I β-turn.

Electrophysiological Experiments with s-Discrepin. To characterize the s-discrepin blockade on the I_A potassium current, electrophysiological experiments with the patch−clamp technique in the whole-cell configuration were performed on rat cerebellum granular cells in culture. As shown in Figure 5, the addition to the standard solution of synthetic peptide at a concentration of 400 nM inhibited the I_A current in an irreversible way. The top frame of Figure 5 shows the two main components of outward K currents present on newborn rat cerebellum granular cells: a fast transient, low-voltage-activated current (I_A), which decays to a steady-state level in ∼100 ms due to the second component, which is similar to the classical noninactivating squid axon potassium current (I_d). The middle frame traces show that s-discrepin inhibited the current at all voltages and that this inhibition was not reversed by perfusing the cells with the control external solution (bottom frame traces). Panel 5B shows the current−voltage relationship of the traces in panel A, where the current recovery was absent or very small after perfusing the neuron with a free peptide solution. Experimental points were measured at the peak value for the I_A current and at the end of the 200 ms pulse for the steady-state I_d current. The s-discrepin shows a much stronger affinity for the I_A-type channel than for the I_d-type channel.

The time course of the current decrease is shown in Figure 6A. Steady-state inhibition was reached rapidly (half-time of ∼1 min). Recovery of the current was very small after washout. The peptide affects K^+ conductance in a dose-dependent manner. In Figure 6B, experimental points were fitted to the Michaelis−Menten equation which gave a half-effective dose IC_{50} of 162 ± 19 nM. Blockade of K^+ permeation was consistent with a 1:1 stoichiometry of binding of s-discrepin to the channel.

Competition Experiments and Liquid-Phase Radioimmunoassay. To further characterize their pharmacological properties, n- and s-discrepin were tested for their ability to modulate the [^{125}I]sBmTX3 binding in rat brain (Figure 7A). Both toxins were able to totally displace [^{125}I]sBmTX3 bound to its receptor site. The half-inhibition (IC_{50}) concentrations observed were 388 pM for BmTX3 and 14 and 23 pM for n- and s-discrepin, respectively.

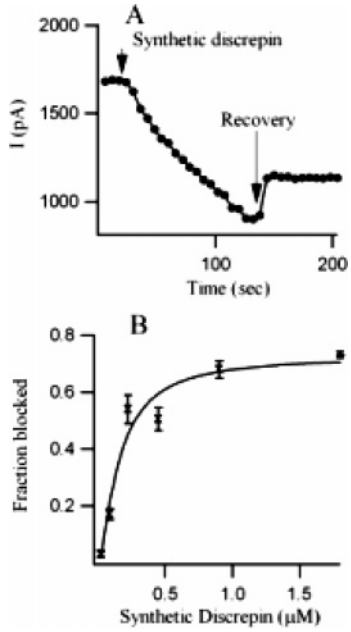

FIGURE 6: Electrophysiological experiments. (A) Time course of s-discrepin response and current recovery after washout. Depolarizing pulses from HP from −80 to 40 mV were repeated every 6 s. Arrows indicate application and washout of s-discrepin. (B) Dose−response curve of the peak current (I_A) vs the synthetic peptide concentration. Data were fitted to the Michaelis−Menten equation (Hill coefficient of 1) ($I_{max} - I)/I_{max} = 1/(1 + IC_{50}/C$), where I_{max} is the control peak current and I is the current after toxin addition. The fitted graph gives a half-effective dose of 162 ± 19 nM.

The specific immune serum obtained from rabbits against BmTX3-delYP was tested for its ability to recognize n-discrepin and its synthetic analogue in a competitive RIA with [^{125}I]BmTX3 (Figure 7B). The IC_{50} value was 800 pM for BmTX3. No cross reactivity was observed between n- or s-discrepin and BmTX3 even at high toxin concentrations (0.1 μM) despite a high degree of sequence similarity of the toxins.

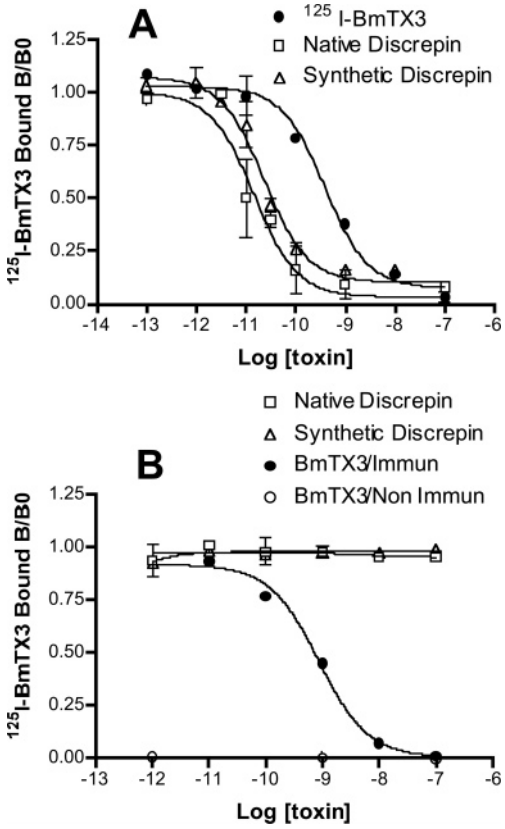

FIGURE 7: Competitive binding to rat brain synaptosomal fraction P2. (A) Displacement of [^{125}I]BmTX3 (40 pM final dilution) bound to its specific binding site on P2 (90 μg/assay) at increasing concentrations of native BmTX3, n-discrepin, and s-discrepin. (B) Competitive liquid-phase radioimmunoassay (RIA). Displacement of [^{125}I]BmTX3 (40 pM final dilution) bound to its specific rabbit serum (final dilution of 1:300000) at increasing concentrations of native BmTX3, n-discrepin, and s-discrepin. Nondiluted preimmune serum was used as a negative control to ensure that nonspecific binding accounted for less than 5% of the total binding (not shown). Results in panels A and B are expressed as the fraction of bound [^{125}I]BmTX3 over the radioactivity in the control (B0). The nonspecific binding was subtracted. For panels A and B, each value was the mean of two independent experiments performed in triplicate. Data were analyzed using PRISM (GraphPad).

DISCUSSION

Scorpion toxins specific for K^+ channels are classified into three families, α-, β-, and γ-scorpion toxins, abbreviated KTx-s, and the largest of them, the α-KTx family, contains at present 20 subfamilies (Y. Abdel-Mottaleb, F. Coronas, A. R. Roodt, L. D. Possani, and J. Tytgat, personal communication). Since classification of the toxins is based on their sequence analysis, proteins belonging to one subfamily can differ in their activities. This does not seems to be the case for the α-KTx15 subfamily as all its members known so far were shown to selectively block A-type K^+ channels. We report here the solution structure of discrepin that represents only ca. 0.2% of the soluble scorpion venom (*1*). The amount of the molecule sufficient for a detailed study was obtained by chemical synthesis and in vitro oxidative folding (s-discrepin) and compared to the peptide purified from the venom (n-discrepin). The comparison of HPLC retention times, molecular masses, one-dimensional spectra obtained at different temperatures, and 2D TOCSY spectra indicated that n- and s-discrepin have effectively the same structure, although differences in the chemical shifts of some amide protons were observed. These do not exceed 0.12 ppm and can be ascribed to differences in conditions such as pH and ionic strength. Moreover, the electrophysiological data described in this work with s-discrepin are fully compatible with the results obtained in a previous paper (*1*) with native discrepin, which blocks fast activating and inactivating K^+ currents in cerebellum granular cells. The physiological action induced by native and synthetic peptides added to an external solution under the same conditions points to an identical molecular mechanism of current inhibition. The peptides reduce the I_A current in a selective manner with practically identical affinity, with half-effective dose IC_{50} values of 190 ± 30 and 162 ± 19 nM for native (*1*) and synthetic discrepin, respectively. The current recovery is not reversible, and long-lasting washing does not remove the blockage. Both peptides do not affect the kinetics of the channel, and the blockage is independent of the test potentials; finally, blocking of K^+ permeability is consistent with the 1:1 stoichiometry of binding of the peptide to the channel. These results suggest the resemblance with the mechanism of blockage described for other Kv channels using charybdotoxin (ChTx) and iberiotoxin (*3*, *38*).

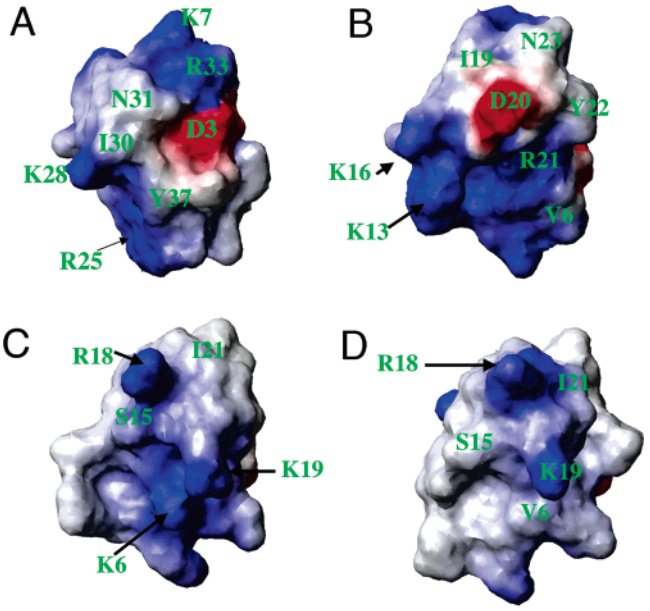

FIGURE 8: Electrostatic surface of discrepin and of two other representatives of the α-Ktx15 subfamily, Aa1 and BmTX3: (A) *β*-sheet face of discrepin, (B) α-helix face of discrepin, (C) α-helix face of Aa1, and (D) α-helix face of BmTx3.

Competition experiments performed with discrepin showed that both n- and s-discrepin fully inhibited the binding of ^{125}I-labeled sBmTx3 to its receptor site in rat brain synaptosomal fraction P2. Similar results were obtained formerly for Aa1 and AmmTx3 in competition experiments against [^{125}I]sBmTx3 (*6*). On the other hand, it was demonstrated that other K^+-channel blockers, namely, the Kv1. family blockers (including ChTx that also blocks the BK_{Ca} channel), Kv3.4 blockers (BDS-I and -II), and HpTx1, a blocker of Kv4.2/Kv4.3, were unable to compete with [^{125}I]sBmTx3 (*6*). The Kv1. family blockers, the BK_{Ca} channel blockers, and the SK_{Ca} blockers were also unable to displace ^{125}I-labeled AmmTx3 from its binding site (*7*). All these results support the hypothesis that discrepin as well as the other molecules of the-KTx15 subfamily could bind to a very specific and unique type of receptor channel. The only feature that distinguishes discrepin from other α-KTx15 toxins is the irreversibility of the A-current inhibition.

The ChTx-like blockage of K_v channels is performed through the interactions with the side chains of residues in, and around, the *β*-sheet face. Inspection of the corresponding electrostatic surfaces calculated for discrepin (Figure 8A) highlights the role of the classical functional dyad targeting K_V channels (*39*) formed in discrepin by Lys28 and Tyr37. The side chains of residues Ile30 and Asn31 from the *β*-turn connecting the second and third antiparallel *β*-strands also contribute to this surface. As demonstrated for other K^+-channel specific toxins (*40*, *41*), residues at positions equivalent to Asn31 of discrepin can discriminate between K_v and BK_{Ca} channels. The Asn residue favors the binding to K_v channels (*40*, *41*). Among other residues contributing to the solvent accessible surface of this face, spatially close Asp3 and Arg33 seem to play a role in stabilizing the overall structure, whereas the side chains of Lys7 and Arg25 situated on the opposite edges of the side might potentially be involved in interactions with still unidentified channel residues. This seems to be most plausible for Arg25. In the recent structural study of the complex between the KcsA channel and charybdotoxin (*42*), the authors underlined the importance of the electrostatic interaction between the charybdotoxin Arg25 and an aspartic residue of the KcsA C chain (Asp64). Although position 25 is not exactly equivalent in ChTx and in discrepin (there is a shift of one residue in their sequence alignment), the positioning of the side chains of Arg25 in space is very similar for both ChTx and discrepin. With the exception of Arg25, which corresponds to Ala24 in the five other members of the α-KTx15 subfamily, almost all the residues forming the functional *β*-face of discrepin are conserved (Figure 1). The Arg25/Ala24 difference could at least partially explain the particularly high affinity of the discrepin for the K^+ channel when compared to the affinities of other toxins of the subfamily. Another substitution in the C-terminal region of discrepin is Thr35 which corresponds to Val34 in all other members of the same subfamily. However, the side chains of these amino acids are buried inside the molecule, as calculated for the discrepin conformers, and for the models of both Aa1 and BmTx3. Thus, it is assumed that these substitutions could hardly play a significant functional role in discriminating distinct functions. Preliminary physiological results obtained with a mutant discrepin in which Thr35 was substituted for Val35 showed no differences in function (G. Prestipino, G. Corzo, and L. D. Possani, unpublished observations).

The lack of cross reactivity between discrepin and BmTX3 in the antiserum specific for BmTX3-delYP that was shown to have the same effective structure as the native peptide (*8*) is possibly due to the fact that the antibodies are directed against the epitope located on the nonconserved part of the molecule.

In fact, the opposite, "α-helix" side of the molecule displays an electrostatic surface reflecting great variability of residues in this part of the α-KTx15 sequences. This face of discrepin is primarily defined by residues Lys13, Lys16, Ile19, Asp20, and Arg21 protruding from the helix, followed by Tyr22 and Asn23 from the turn connecting the helix to the second *β*-strand. Val6 located on the first *β*-strand also contributes to the surface. Electrostatic features of this surface are different when discrepin, Aa1, and BmTX3 are compared (Figure 8B−D and Figure 1). The positively charged patch formed by Lys13, an insertion in the sequence of discrepin, and its Lys16 is absent from the surface of both Aa1 and BmTx3. Discrepin is the only peptide of the α-KTx15 subfamily presenting an acidic residue, Asp20, at this side of the molecule, although its negative charge might be to some extent attenuated by interactions with the side chains of the neighboring Arg21. These two discrepin residues are substituted in the other members of the subfamily with Arg19 and Val/Ala20, respectively, whereas the sequence equivalent of discrepin Ile19 is Arg18. These differences could account for the possible recognition of other channels, according to a publication by Huys et al. (*43*). These authors suggested that Arg18 together with Lys19 in BmTX3 might explain its activity on HERG channels. Such a positively charged pair of residues is missing at the equivalent location in discrepin. The discrepin Lys13 and Lys16 pair, although similarly close in space, is however located in a different position.

Discrepin, targeting the voltage-dependent K^+ channel expressing A-type currents in cerebellum granular cells, is

expected to reveal more about the role of these channels in neural and cardiac tissues. Since physiological studies have shown that A-type currents exhibit a wide range of biophysical and pharmacological properties according to their cellular function related to molecular heterogeneity, the characterization of new peptides which target A-type currents is essential for dissecting the currents carried out from different A-type K^+ channels. It will be valuable to find molecular tools affecting selectively Kv1.4, -3.4, -4.1, -4.2, and -4.4 channels which are known to express A-type K^+ currents. Thus, the search for and characterization of new members of toxins active on this subtype of K^+ channels and the construction of synthetic peptides and site specific mutants of these toxins represent an important tool in studying ion-channel function. Indeed, the knowledge of the interacting surfaces between the channels and toxins will be vital for the rational design of more specific drugs and the control of pathologies associated with K^+ channels.

ACKNOWLEDGMENT

We thank Dr. Inaki Guijarro for helpful discussions.

SUPPORTING INFORMATION AVAILABLE

Chemical shifts of all protons of n- and s-discrepin. This material is available free of charge via the Internet at http://pubs.acs.org.

REFERENCES

1. D'Suze, G., Batista, C. V., Frau, A., Murgia, A. R., Zamudio, F. Z., Sevcik, C., Possani, L. D., and Prestipino, G. (2004) Discrepin, a new peptide of the sub-family α-ktx15, isolated from the scorpion *Tityus discrepans* irreversibly blocks K^+-channels (IA currents) of cerebellum granular cells, *Arch. Biochem. Biophys. 430*, 256−63.
2. Coetzee, W. A., Amarillo, Y., Chiu, J., Chow, A., Lau, D., McCormack, T., Moreno, H., Nadal, M. S., Ozaita, A., Pountney, D., Saganich, M., Vega-Saenz de Miera, E., and Rudy, B. (1999) Molecular diversity of K^+ channels, *Ann. N.Y. Acad. Sci. 868*, 233−85.
3. Rodriguez de la Vega, R. C., and Possani, L. D. (2004) Current views on scorpion toxins specific for K^+-channels, *Toxicon 43*, 865−75.
4. Tytgat, J., Chandy, K. G., Garcia, M. L., Gutman, G. A., Martin-Eauclaire, M. F., van der Walt, J. J., and Possani, L. D. (1999) A unified nomenclature for short-chain peptides isolated from scorpion venoms: α-KTx molecular subfamilies, *Trends Pharmacol. Sci. 20*, 444−7.
5. Sanguinetti, M. C., Johnson, J. H., Hammerland, L. G., Kelbaugh, P. R., Volkmann, R. A., Saccomano, N. A., and Mueller, A. L. (1997) Heteropodatoxins: Peptides isolated from spider venom that block Kv4.2 potassium channels, *Mol. Pharmacol. 51*, 491−8.
6. Vacher, H., Romi-Lebrun, R., Mourre, C., Lebrun, B., Kourrich, S., Masmejean, F., Nakajima, T., Legros, C., Crest, M., Bougis, P. E., and Martin-Eauclaire, M. F. (2001) A new class of scorpion toxin binding sites related to an A-type K^+ channel: Pharmacological characterization and localization in rat brain, *FEBS Lett. 501*, 31−6.
7. Vacher, H., Alami, M., Crest, M., Possani, L. D., Bougis, P. E., and Martin-Eauclaire, M. F. (2002) Expanding the scorpion toxin α-KTX 15 family with AmmTX3 from *Androctonus mauretanicus*, *Eur. J. Biochem. 269*, 6037−41.
8. Vacher, H., Prestipino, G., Crest, M., and Martin-Eauclaire, M. F. (2004) Definition of the α-KTx15 subfamily, *Toxicon 43*, 887−94.
9. Diochot, S., Drici, M. D., Moinier, D., Fink, M., and Lazdunski, M. (1999) Effects of phrixotoxins on the Kv4 family of potassium channels and implications for the role of Ito1 in cardiac electrogenesis, *Br. J. Pharmacol. 126*, 251−63.
10. Bernard, C., Legros, C., Ferrat, G., Bischoff, U., Marquardt, A., Pongs, O., and Darbon, H. (2000) Solution structure of hpTX2, a toxin from *Heteropoda venatoria* spider that blocks Kv4.2 potassium channel, *Protein Sci. 9*, 2059−67.
11. Escoubas, P., Diochot, S., Celerier, M. L., Nakajima, T., and Lazdunski, M. (2002) Novel tarantula toxins for subtypes of voltage-dependent potassium channels in the Kv2 and Kv4 subfamilies, *Mol. Pharmacol. 62*, 48−57.
12. Diochot, S., Schweitz, H., Beress, L., and Lazdunski, M. (1998) Sea anemone peptides with a specific blocking activity against the fast inactivating potassium channel Kv3.4, *J. Biol. Chem. 273*, 6744−9.
13. Pisciotta, M., Coronas, F. I., Possani, L. D., and Prestipino, G. (1998) The *Androctonus australis* garzoni scorpion venom contains toxins that selectively affect voltage-dependent K^+-channels in cerebellum granular cells, *Eur. Biophys. J. 27*, 69−73.
14. Legros, C., Bougis, P. E., and Martin-Eauclaire, M. F. (2003) Characterisation of the genes encoding Aa1 isoforms from the scorpion *Androctonus australis*, *Toxicon 41*, 115−9.
15. Corzo, G., Escoubas, P., Villegas, E., Karbat, I., Gordon, D., Gurevitz, M., Nakajima, T., and Gilles, N. (2005) A Spider Toxin That Induces a Typical Effect of Scorpion α-Toxins but Competes with β-Toxins on Binding to Insect Sodium Channels, *Biochemistry 44*, 1542−9.
16. States, D. J., Haberkorn, R. A., and Ruben, D. J. (1982) A two-dimensional nuclear Overhauser experiment with pure absorption phase in four quadrants, *J. Magn. Reson. 48*, 286−92.
17. Piantini, U., Sørensen, O. W., and Ernst, R. R. (1982) Multiple quantum filters for elucidating NMR coupling networks, *J. Am. Chem. Soc. 104*, 6800−1.
18. Rance, M., Sørensen, O. W., Bodenhausen, G., Wagner, G., Ernst, R. R., and Wüthrich, K. (1983) Improved spectral resolution in COSY ^{1}H NMR spectra of proteins via double quantum filtering, *Biochem. Biophys. Res. Commun. 117*, 479−85.
19. Boyd, J., Dobson, C. M., and Redfield, C. (1983) Correlation of proton chemical shifts in proteins using two-dimensional double-quantum spectroscopy, *J. Magn. Reson. 55*, 170−6.
20. Griesinger, C., Otting, G., Wüthrich, K., and Ernst, R. R. (1988) Clean TOCSY for ^{1}H spin system identification in macromolecules, *J. Am. Chem. Soc. 110*, 7870−2.
21. Kumar, A., Ernst, R. R., and Wuthrich, K. (1980) A two-dimensional nuclear Overhauser enhancement (2D NOE) experiment for the elucidation of complete proton−proton cross-relaxation networks in biological macromolecules, *Biochem. Biophys. Res. Commun. 95*, 1−6.
22. Levitt, M. H., Freeman, R., and Frenkiel, T. (1982) Broadband heteronuclear decoupling, *J. Magn. Reson. 47*, 328−30.
23. Bax, A., and Davis, D. G. (1985) MLEV-17-based two-dimensional homonuclear magnetization transfer spectroscopy, *J. Magn. Reson. 65*, 355−60.
24. Wishart, D. S., and Sykes, B. D. (1994) Chemical shifts as a tool for structure determination, *Methods Enzymol. 239*, 363−92.
25. Wishart, D. S., Sykes, B. D., and Richards, F. M. (1992) The chemical shift index: A fast and simple method for the assignment of protein secondary structure through NMR spectroscopy, *Biochemistry 31*, 1647−51.
26. Wüthrich, K. (1986) in *NMR of proteins and nucleic acids*, John Wiley & Sons, New York.
27. Bartels, C., Xia, T.-H., Billeter, M., Güntert, P., and Wüthrich, K. (1995) The program XEASY for computer-supported NMR spectral analysis of biological macromolecules, *J. Biomol. NMR 6*, 1−10.
28. Linge, J. P., O'Donoghue, S. I., and Nilges, M. (2001) Automated assignment of ambiguous nuclear overhauser effects with ARIA, *Methods Enzymol. 339*, 71−90.
29. Brunger, A. T., Adams, P. D., Clore, G. M., DeLano, W. L., Gros, P., Grosse-Kunstleve, R. W., Jiang, J. S., Kuszewski, J., Nilges, M., Pannu, N. S., Read, R. J., Rice, L. M., Simonson, T., and Warren, G. L. (1998) *Crystallography & NMR system*: A new software suite for macromolecular structure determination, *Acta Crystallogr. D54*, 905−21.
30. Koradi, R., Billeter, M., and Wüthrich, K. (1996) MOLMOL: A program for display and analysis of macromolecular structures, *J. Mol. Graphics 14*, 51−5.
31. Laskowski, R. A., MacArthur, M. W., Moss, D. S., and Thornton, J. M. (1993) PROCHECK: A program to check the stereochemical quality of protein structures, *J. Appl. Crystallogr. 26*, 283−91.

32. Hooft, R. W., Vriend, G., Sander, C., and Abola, E. E. (1996) Errors in protein structures, *Nature 381*, 272.
33. Marti-Renom, M. A., Madhusudhan, M. S., and Sali, A. (2004) Alignment of protein sequences by their profiles, *Protein Sci. 13*, 1071−87.
34. Berman, H. M., Westbrook, J., Feng, Z., Gilliland, G., Bhat, T. N., Weissig, H., Shindyalov, I. N., and Bourne, P. E. (2000) The Protein Data Bank, *Nucleic Acids Res. 28*, 235−42.
35. Vacher, H., and Martin-Eauclaire, M. F. (2004) Antigenic polymorphism of the "short" scorpion toxins able to block K^+ channels, *Toxicon 43*, 447−53.
36. Levi, G., Aloisi, F., Ciotti, M. T., and Gallo, V. (1984) Autoradiographic localization and depolarization-induced release of acidic amino acids in differentiating cerebellar granule cell cultures, *Brain Res. 290*, 77−86.
37. Hamill, O. P., Marty, A., Neher, E., Sakmann, B., and Sigworth, F. J. (1981) Improved patch-clamp techniques for high-resolution current recording from cells and cell-free membrane patches, *Pfluegers Arch. 391*, 85−100.
38. Garcia, M. L., Hanner, M., and Kaczorowski, G. J. (1998) Scorpion toxins: Tools for studying K^+ channels, *Toxicon 36*, 1641−50.
39. Dauplais, M., Lecoq, A., Song, J., Cotton, J., Jamin, N., Gilquin, B., Roumestand, C., Vita, C., de Medeiros, C. L., Rowan, E. G., Harvey, A. L., and Menez, A. (1997) On the convergent evolution of animal toxins. Conservation of a diad of functional residues in potassium channel-blocking toxins with unrelated structures, *J. Biol. Chem. 272*, 4302−9.
40. Goldstein, S. A., Pheasant, D. J., and Miller, C. (1994) The charybdotoxin receptor of a Shaker K^+ channel: Peptide and channel residues mediating molecular recognition, *Neuron 12*, 1377−88.
41. Ranganathan, R., Lewis, J. H., and MacKinnon, R. (1996) Spatial localization of the K^+ channel selectivity filter by mutant cycle-based structure analysis, *Neuron 16*, 131−9.
42. Yu, L., Sun, C., Song, D., Shen, J., Xu, N., Gunasekera, A., Hajduk, P. J., and Olejniczak, E. T. (2005) Nuclear magnetic resonance structural studies of a potassium channel-charybdotoxin complex, *Biochemistry 44*, 15834−41.
43. Huys, I., Xu, C. Q., Wang, C. Z., Vacher, H., Martin-Eauclaire, M. F., Chi, C. W., and Tytgat, J. (2004) BmTx3, a scorpion toxin with two putative functional faces separately active on A-type K^+ and HERG currents, *Biochem. J. 378*, 745−52.

BI0519248